Tests for equilibration of ^{149}Tb* composite nuclei produced in the reactions 337 MeV ^{40}Ar + ^{nat}Ag and 640 MeV ^{86}Kr + ^{63}Cu

J. Boger,* John M. Alexander, Roy A. Lacey, and A. Narayanan†
Department of Chemistry, State University of New York at Stony Brook, Stony Brook, New York 11794
(Received 28 April 1993)

Experimental results are compared for the two matched heavy ion reactions 337 MeV ^{40}Ar + ^{nat}Ag and 640 MeV ^{86}Kr + ^{63}Cu as a test of the extent of equilibration of the intermediate composite nucleus ^{149}Tb*(E^* = 194 MeV). Spin zones associated with the evaporation residues (ER) are found to agree well for these entrance channels. Agreement is not as close for the fission class due to the inclusion of deeply inelastic reactions (DIR) along with fusion-fission (FF) for the ^{86}Kr reaction. Inclusive and coincidence measurements of energy spectra and angular distributions for the light charged particles indicate that these reactions produce composite nuclei with similar temperatures, spins, and moments of inertia. The energy spectra for both reactions are identically shifted relative to statistical model calculations. This suggests that the composite nuclei are highly distended prior to their cooling by particle evaporation. Multiplicities also agree for ^{1}H and ^{4}He production in association with the ER and FF reaction classes. It is noteworthy that prescission ^{1}H and ^{4}He multiplicities are in such good agreement, because the magnitude of these multiplicities seems to be dictated by the dynamical time scale of the fission process. That these prescission multiplicities are large suggests that the fission time scale is slow relative to particle evaporation; that they match for these reactions indicates that this is an equilibrium property of the intermediate composite nuclei. We conclude that extensive and rapid thermalization and shape equilibration have occurred despite estimates that the nuclear relaxation time and decay lifetime are nearly the same.

PACS number(s): 24.60.Dr, 25.70.Gh, 25.70.Jj

I. INTRODUCTION

Heavy ion reactions are routinely used to produce composite nuclei with large angular momenta and excitation energies. In the energy region of $E/A \leq 10$ MeV essentially complete fusion and deeply inelastic reactions comprise much of the the total reaction cross section and are the major sources of light particle production. Over the past few years, there has been strong interest directed toward inferring the statistical properties of these hot, rapidly rotating emitters (see, for example, Refs. [1] and [2] and references therein). Particle-particle and fragment-particle coincidence measurements have allowed identification of the mechanistic sources of these light particles. Light charged particles have proved to be effective probes of their emitters and have provided information on nuclear temperatures, shapes, moments of inertia, and particle multiplicities.

Such a detailed picture of these nuclei now offers an opportunity to test the extent of many facets of their equilibration. An important question then is, does thermalization occur rapidly enough so that the temperatures, shapes, particle multiplicities, etc., are equilibrium properties of these hot, highly unstable nuclei? We may rephrase the question as, how do the nuclear relaxation times compare with the decay lifetime? If the relaxation time exceeds the lifetime of the composite nucleus, then fast, preequilibrium reactions may dominate.

The nuclear lifetime may be estimated from the statistical model [3]

$$\tau \simeq \tau_n \simeq \frac{200}{U - B_n} \frac{\rho_c(U)}{\rho_n(U - B_n)} \simeq \frac{200}{U - B_n} e^{B_n/T} \frac{\rho_c(U)}{\rho_n(U)}. \tag{1.1}$$

Equation (1.1) assumes that the emitted particle is a neutron; τ is the lifetime of the nucleus in units of $(2R/c)$, R, T, and U are the radius, temperature, and initial internal energy of the composite nucleus, B_n is the binding energy of the neutron, and $\rho_c(U)$ and $\rho_n(U-B_n)$ are the level densities of the composite and daughter nuclei, respectively.

For the ^{149}Tb composite nucleus (E^* = 194 MeV) produced in the two reactions reported here, the lifetime is estimated to be $\approx 12(2R/c)$. The relaxation time, on the other hand, is estimated to be about $(5\text{–}10)(2R/c)$ [4]. Although these estimates are crude, we see that the estimates for relaxation time and decay lifetime are quite close. Understanding the extent of equilibration can provide insight into the relative lengths of these time scales.

For rapidly rotating nuclei, the interplay between relaxation time and decay lifetime also plays a role in dic-

*Present address: Texas A&M University, Cyclotron Institute, College Station, TX 77843-3366.
†Present address: Department of Chemistry, Brock University, St. Catherines, Ontario, Canada L253A1.

tating how the system decays. But what if these time scales are longer than the time scale for fission? In the framework of the rotating liquid drop model, one expects the barrier for symmetric fission to vanish for nuclei with sufficiently high spins. For such a case, the Coulomb and centrifugal forces may rapidly drive the fragments apart with little or no regard to the phase space of the system. However, it is now known that a large amount of composite nucleus evaporation of light particles occurs prior to fission, even for nuclei of medium mass ($A \approx 150$). This has been a surprising result of the research in recent years. Observations of near-scission ^{4}He emission [5], nuclear shadowing [5], and prescission neutron multiplicities [6,7] have been used as "clocks" to estimate the fission time scale. Such results indicate that the fission process proceeds rather slowly, at least slower than the evaporation of light particles. For this situation the phase space of a partially equilibrated nucleus may drive its decay even while it undergoes fission.

In this paper we compare results from two reactions: 337 MeV ^{40}Ar + ^{nat}Ag and 640 MeV ^{86}Kr + ^{63}Cu. Both reactions produce the composite nucleus ^{149}Tb* with an initial excitation energy of 194 MeV and lead to substantial residue and fission cross sections. Experimental results from the ^{40}Ar entrance channel have been previously published [5,8]. Results from the ^{86}Kr reaction are reported in Refs. [9–12]. We first compare spin zones [8,13–17] associated with the reaction cross sections leading to evaporation residues (ER's) and fusion-fission (FF) for these two entrance channels. Next we use ^{1}H and ^{4}He emission as probes of equilibration by examining their spectral shapes, angular distributions, particle-emission barriers, and multiplicities associated with both the ER and FF reaction classes. It has been shown that particle-particle coincidence events in this regime [5,18] are primarily associated with the ER's. They are therefore excellent probes of the most central collisions between target and projectile. Cross sections for the subset of ^{1}H and ^{4}He emission from the ER's are also derived. Examination of the data leads to the conclusion that extensive thermalization of these nuclei has occurred despite the estimate that the relaxation time and decay lifetimes are not very different.

II. OVERVIEW OF REACTION CLASSES

Cross sections for the ER and FF reaction classes [including deeply inelastic reactions (DIR)] have been measured for the reactions ^{86}Kr + ^{65}Cu [15–17] and ^{40}Ar + ^{nat}Ag [5,13–16]. Excitation functions from the combined results of these works and our own are presented in Fig. 1.

A. Fusion and the formation of evaporation residues

Figure 1(a) shows several excitation functions, σ_{ER} (lower curve) and $\sigma_{ER}+\sigma_{FF}$ (upper curve). At the lowest energies, only ER's are formed. As the excitation energy increases, the fission process appears and σ_{FF} becomes an appreciable part of the total reaction cross section. The ER cross section reaches a broad maximum and then levels off and even decreases. Similar results are found for the ^{86}Kr reactions shown in the lower curve of Fig. 1(b).

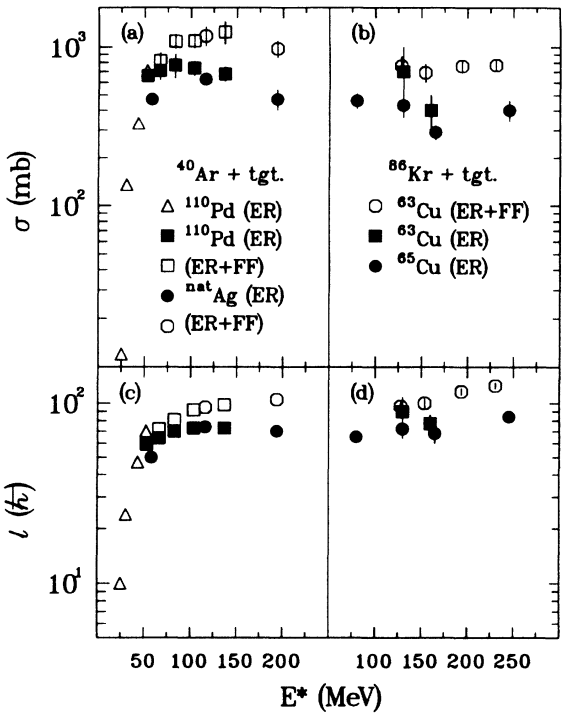

FIG. 1. (a) ER and ER + FF cross sections as functions of the excitation energy for the reactions ^{40}Ar + ^{nat}Ag(^{110}Pd). (b) Same for ^{86}Kr + ^{63}Cu(^{65}Cu). (c) Dependence of angular momentum ℓ on the excitation energy for the reactions in (a). (d) Same but for the ^{86}Kr-induced reactions. The references are [5, 12–17] and this work.

To each reaction class, spin zones may be assigned by equating an experimental cross section (σ_{ER}, σ_{FF}, etc.) to a summation over the partial waves employed in producing that cross section. For example, one may write

$$\sigma_{fus} = \sigma_{ER} + \sigma_{FF} = \pi\lambda^2 \sum_{\ell=0}^{\ell_{ER}} (2\ell+1)T_\ell + \pi\lambda^2 \sum_{\ell=\ell_{ER}}^{\ell_{ER+FF}} (2\ell+1)T_\ell, \quad (2.1)$$

where σ_{fus} is the fusion cross section, λ is the projectile wavelength, and T_ℓ is the transmission coefficient. We obtain values of ℓ_{ER} from σ_{ER} by using the sharp cutoff approximation such that the transmission coefficient is either 0 or 1.

Solid points in Fig. 1(c) show the variation of ℓ_{ER} with excitation energy for the ^{40}Ar-induced reactions. We observe a sharp initial increase in ℓ_{ER} and then a plateau at a value of $\approx 70\hbar$. It would seem that this value of $70\hbar$ is related to the limiting angular momentum for the production of ER's. Composite nuclei produced with angular momentum much greater than $70(\pm 3)\hbar$ decay predominantly by fission or by a fast fissionlike process. This value of ℓ_{ER} is consistent with predictions of the rotating liquid drop model [19].

The lower curve in Fig. 1(d) is similar to that for Fig. 1(c). It reveals that for the ^{86}Kr + ^{63}Cu entrance channel, ℓ_{ER} levels off at $\approx 75(\pm 5)\hbar$. This value is equivalent, within experimental uncertainties, to that for the ^{40}Ar reaction. It would seem that the angular momentum at which fission becomes the preferred decay path is an equilibrium property of the fused system.

B. Fusion-fission

Now consider the FF reaction class. Figure 1(a) shows that σ_{ER+FF} for the ^{40}Ar reactions reaches a broad maximum and then slowly tapers off. This resembles the behavior of the ER reaction class. The upper curve in Fig. 1(c) shows that the entrance channel ℓ value saturates at $\approx 101\hbar$ for ℓ_{ER+FF}. One can say that those ℓ waves between $70\hbar$ and $101\hbar$ lead to composite nuclei that predominantly undergo fission. The downward slopes of the excitation functions in Fig. 1(a) for σ_{ER} and σ_{ER+FF} are therefore governed by the decrease in $\pi(\frac{\lambda}{2\pi})^2$ as the bombarding energy increases.

In Fig. 1(b) we see that for ^{86}Kr the ER + FF cross section continues to increase slightly as the energy increases. Furthermore, as indicated in Fig. 1(d), the associated maximum ℓ value ($\ell_{ER+FF/DIR}$) also continues to increase with an increase in energy. This behavior departs from that observed for the ^{40}Ar-induced reactions and may be ascribed to the inclusion of some DIR reactions for the nearly mass-symmetric entrance channel of the ^{86}Kr reactions. The so-called FF cross sections for both reactions shown in Fig. 1 are measured for $24 \leq Z \leq 40$. For the ^{40}Ar reactions, these cross sections are expected to be essentially free from projectilelike or targetlike fragments. However, the cross sections measured for the ^{86}Kr reactions most likely include some projectilelike or targetlike fragments, and therefore these entrance channels probably include some higher ℓ waves as well as the same ensemble of nuclei for the FF reaction class. Nevertheless, it seems that a common intermediate composite nucleus can be said to have fixed the upper limit to the angular momentum for ER production.

III. LIGHT CHARGED PARTICLES AS PROBES OF EQUILIBRATION

A. Energy spectra

We now look at the light charged particles produced from these two entrance channels. Figure 2(a) shows inclusive ^{4}He energy spectra from both the ^{40}Ar (histograms) and ^{86}Kr (points) reactions. The center of mass (c.m.) angles are indicated for the ^{86}Kr reaction. For the ^{40}Ar reaction, the c.m. angles have been reflected into the forward hemisphere by subtraction from π. This gives the equivalent angle for a reaction that employs reversed kinematics. In all cases the values of $\theta_{c.m.}$ for the ^{40}Ar reaction differ by no more than 5° from those for the ^{86}Kr reaction.

The ^{4}He energy spectrum from the ^{86}Kr reaction was

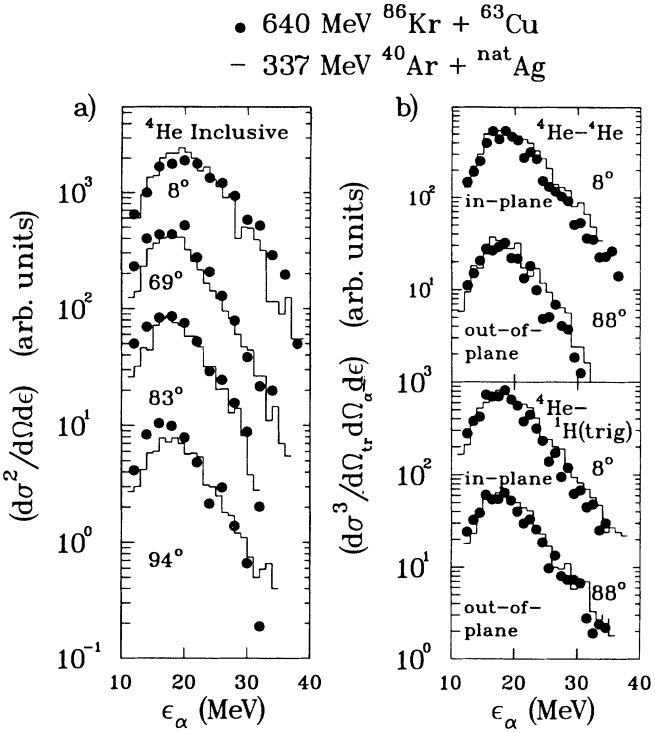

FIG. 2. Comparison of ^{4}He energy spectra for 337 MeV ^{40}Ar + ^{nat}Ag (histograms) and 640 MeV ^{86}Kr + ^{63}Cu (points). Inclusive c.m. energy spectra are shown in (a), and in coincidence with ^{4}He and ^{1}H triggers ($\theta_{c.m.} \approx 90°$) in (b). The inclusive spectra have been normalized at 83°. Indicated angles are for the ^{86}Kr reaction. Angles for the ^{40}Ar reaction are reflected into the forward hemisphere with respect to the beam. In-plane and out-of-plane coincidences are shown in (b). Spectra have been individually peak normalized.

peak normalized to that for the ^{40}Ar reaction at $\theta_{c.m.} = 83°$. This normalization factor was then applied to the other ^{86}Kr spectra. We observe at all angles a good match in spectral shape, especially on the high energy side, though somewhat less on the low energy side. This may be attributed to differences in the fragment emission, as these spectra include emission from all the various sources. The shapes of the spectra are Maxwellian. Furthermore, the average energies are nearly invariant with angle. This is consistent with almost isotropic emission from a single dominant source moving with the c.m. velocity.

Prethermalization emission (PTE) was not observed for the ^{86}Kr reaction possibly due to the placement of the detectors, which were set at forward laboratory angles or at backward angles with respect to the direction of the light reaction partner in the rest frame of the two-body system, viz., ^{63}Cu. PTE was, however, observed in the ^{40}Ar reaction at forward laboratory angles [5]. Particle energy spectra that include PTE have high apparent temperatures unlike those shown in Fig. 2(a) for either entrance channel. The similar shapes and low thermal slopes of these spectra give strong evidence for emission predominantly from equilibrated sources.

Figure 2(b) shows ^{4}He energy spectra in coincidence with either an in-plane or out-of-plane ^{4}He or ^{1}H trig-

ger. Trigger angles in the c.m. were ~90°, and all spectra were individually peak normalized. We find that the spectral shapes for the two entrance channels are in very good agreement, both on the low and high energy sides of the peak values. Previous work [5] has shown for the ^{40}Ar reaction that ~86% of the ^{4}He-^{4}He coincidence cross section is derived from composite nuclei that decay to ER's. Similar results have been found for the ^{1}H-^{4}He and ^{1}H-^{1}H cross sections [10]. We infer that energy spectra observed from particle-particle coincidences represent emission predominantly from a single source. This lends support to the conclusion that the lack of agreement on the low energy side of the inclusive spectra is due to fragment emission. Furthermore, thermalization of the fused system is indicated by the similar spectral shapes (and therefore temperatures) produced by these two entrance channels.

B. Angular distributions

Figure 3 shows angular distributions for dimensionless differential cross sections for ^{4}He emission in singles measurements as well as in coincidence with in-plane and out-of-plane ^{4}He and ^{1}H triggers. We note in Fig. 3 that the in-plane cross sections for ^{4}He-^{4}He are somewhat smaller for the ^{86}Kr reaction relative to the ^{40}Ar reaction. However, the anisotropy in the angular distribution is essentially the same for both entrance channels. The anisotropies in the other angular distributions also match rather well.

The statistical evaporation model in its simplest form [3,20,21] predicts the following probability $W(\theta)$ for a nucleus to emit a particle at angle θ with respect to the beam:

$$W(\theta) \propto \exp(-\tfrac{1}{2}\beta_2 \sin^2\theta)\mathbf{I}_0(\tfrac{1}{2}\beta_2 \sin^2\theta), \qquad (3.1)$$

where the anisotropy parameter β_2 is

$$\beta_2 = \frac{\hbar^2 J^2}{2\Im_D T}\left(\frac{\mu R^2}{\Im_D + \mu R^2}\right). \qquad (3.2)$$

The temperature of the daughter nucleus is represented by T, $\Im_D$ is the moment of inertia of the daughter nucleus, μ is the reduced mass of the two-body system, and R is the separation distance between the center of the daughter nucleus and the particle on its surface. The symbol $\mathbf{I}_0$ denotes the zeroth-order Bessel function. Agreement between the various anisotropies in Fig. 3 demands that the effective average value of β_2 for these reactions be very similar, as it is this parameter that drives the angular distributions.

Since the majority of these particles are emitted by nuclei that decay to ER's, we infer from Fig. 1 that the ER spin zones must be well matched for these entrance channels. The temperatures of the daughter nuclei produced in these reactions must also be similar; otherwise, the spectral shapes would not agree as well as they do, as indicated by the energy spectra in Fig. 2. We therefore conclude that similar nuclear shapes are produced in these reactions. This follows from Eq. (3.2). If J and T are equivalent for these two entrance channels, then the values of $\Im_D$ must agree. Furthermore, this conclusion is consistent with the energy spectra in Fig. 2. If the Coulomb barriers to ^{1}H and ^{4}He production differed as they would for emitters of different shape (or $\Im_D$), then the spectra would be shifted in energy with respect to one another. This pattern of results strengthens our conclusion that very similar intermediate composite nuclei are formed in these matched reactions; i.e., their temperatures, spins, and moments of inertia are essentially the same.

C. Reduced barriers

Figure 4(a) shows energy spectra for ^{4}He, ^{3}H, ^{2}H, and ^{1}H in coincidence with ^{4}He for the ^{40}Ar reaction [8]. The histograms represent the experimental spectra; the smooth curves are statistical model (GANES) [22] simulations of these spectra using empirical ^{1}H and ^{4}He fusion barriers for cold spherical nuclei [23]. Note that the

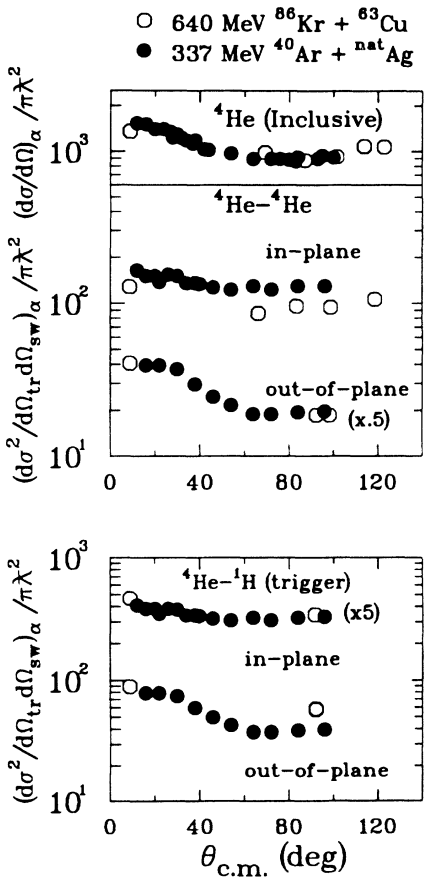

FIG. 3. (a) Angular distributions for dimensionless differential cross sections for inclusive ^{4}He and in coincidence with in plane and out-of-plane ^{4}He triggers ($\theta_{c.m.} \approx 90°$). Open points are for the reaction 337 MeV ^{40}Ar + ^{nat}Ag; solid points for 640 MeV ^{86}Kr + ^{63}Cu. (b) Same, but for in-plane and out-of-plane ^{1}H triggers. Statistical uncertainties are smaller than points.

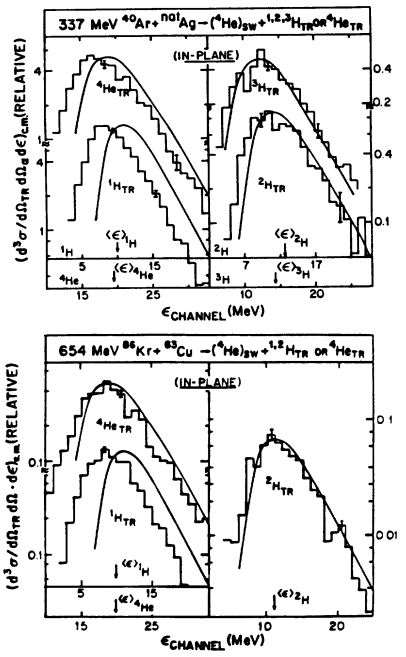

FIG. 4. (a) ^{1,2,3}H and ^{4}He energy spectra in coincidence with ^{4}He for the reaction 337 MeV ^{40}Ar + ^{nat}Ag [8]. Histograms are the experimental spectra, and solid curves are statistical model reaction simulations using cold fusion barriers for spherical emitters [23]. (b) The same for the ^{86}Kr + ^{63}Cu reaction.

experimental energy spectra are shifted to lower values with respect to these simulations in all cases except for ^{3}H. The ^{1}H experimental spectrum is shifted the most, then the ^{4}He, and finally ^{2}H.

Similar shifts are observed for the ^{86}Kr entrance channel shown in Fig. 4(b). In both cases the ^{1}H energy spectra are shifted by approximately 25% relative to those calculated for a spherical emitter. For the ^{4}He spectra one also observes a shift of $\approx$15% for both entrance channels, less than that for ^{1}H. For ^{2}H, the shift is only about 5%. In any case, it would appear these energy shifts occur for both entrance channel reactions.

It can be inferred from these shifts that the composite nucleus ^{149}Tb* has undergone the same size-shape evolution regardless of the different mass asymmetries involved in the entrance channels. Such shifts in energy have on occasion been attributed to deformation of the emitters. However, Lacey *et al.* [8] have shown that nuclear deformation is not enough to explain the magnitudes of these shifts. The suggestion was made that an expanded nuclear stratosphere may be required [8,24–26]. This nuclear stratosphere would presumably result from the expansion of the hot nuclear system. As it cools by the evaporation of particles, it could shrink back to the density characteristic of cold nuclei. Such a shrinking process might be expected to occur rapidly under dynamical (as opposed to statistical) control, but it is noteworthy that these results suggest a common sequence for different entrance channel reactions.

The simulated particle spectra shown in Fig. 4 have been produced by the equivalent one-step statistical model code GANES [22]. The deexcitation of a composite nucleus actually involves the emission of a large number of particles from a chain of emitters. This could lead to an overestimation of the average barrier if the particular particle of interest were to be preferentially emitted at the end of the chain [27]. Calculations that compare equivalent one-step versus multistep calculations have shown that the simulated spectra are essentially identical for these systems [28,29]. Thus it seems that the large shifts in energy shown in Fig. 4 can be attributed to an emitter size or shape that strongly departs from those for cold spherical nuclei.

IV. COMPARISON OF ^{1}H AND ^{4}He MULTIPLICITIES IN ER AND FF/DIR REACTIONS

A. ^{1}H and ^{4}He multiplicities for FF/DIR

In the accompanying paper [10], we report light charged particle multiplicities for composite emission (CE) and fragment emission (FE). A comparison of these multiplicities for these two entrance channels provides an additional test for equilibration of these nuclei in the spin zone of $\approx (70-100)\hbar$. Furthermore, the magnitude of these multiplicities may give insight into the length of the lifetime of the composite nucleus relative to the time it takes to fission.

The multiplicity for a proton from source X is defined as

$$\langle m^p(X)\rangle = \frac{\{\int(\frac{d^2\sigma}{d\Omega_{sw}d\Omega_{tr}})d\Omega_{sw}\}^p}{\{(\frac{d\sigma}{d\Omega_{tr}})\}^X_s} = \frac{\sigma^p(X)}{\sigma_s(X)}, \quad (4.1)$$

where the subscript s denotes the singles mode, tr denotes trigger, and sw the sweeper detector. The method to obtain these multiplicities from the energy spectra from fragment-particle coincidences is given in [5,9,10,30].

As the ^{40}Ar + ^{nat}Ag reaction is mass asymmetric in the entrance channel, it is possible to identify and to separate FF and DIR fragments and obtain their respective multiplicities [5] for both fragment and composite emission. For the ^{86}Kr reaction this separation has not been possible. Therefore, in order to make a comparison between these two entrance channels, it is necessary to combine the separate FF and DIR multiplicities for the ^{40}Ar reaction. The combined FF and DIR multiplicity for composite emission (CE) can then be written as

$$\langle m^p(\mathrm{CE})\rangle = \frac{\sigma(\mathrm{FF})\langle m^p(\mathrm{CE})\rangle + \sigma(\mathrm{DIR})\langle m^p(\mathrm{CE})\rangle}{\sigma(\mathrm{FF})+\sigma(\mathrm{DIR})} \quad (4.2)$$

and similarly for fragment emission (FE),

$$\langle m^p(\mathrm{FE})\rangle = \frac{\sigma(\mathrm{FF})\langle m^p(\mathrm{FE})\rangle + \sigma(\mathrm{DIR})\langle m^p(\mathrm{FE})\rangle}{\sigma(\mathrm{FF})+\sigma(\mathrm{DIR})}. \quad (4.3)$$

The separate multiplicity values for the ^{40}Ar reaction [as well as σ(FF) and σ(DIR)] for each source may be found in [5,8].

Figure 5 provides a bar graph of ^{1}H (p) and ^{4}He (a) multiplicities for the total, ER, and combined FF/DIR reaction classes. The ER particle multiplicities are discussed in the next section. For now, focus on the FF/DIR reaction class. This class is further subdivided into composite emission (CE) and fragment emission (FE) multiplicities. The solid (open) bars are for the ^{86}Kr (^{40}Ar) reaction. The magnitudes of all these multiplicities agree well. Note that even for the FF/DIR reaction class, the CE multiplicities for ^{1}H and ^{4}He emission are in agreement. They are also surprisingly large, if one recalls that these composite emitters have spins well above the critical spin (ℓ_{ER}) for which the fission barrier is expected to vanish [19]. This suggests that the voyage of the unstable composite system to the scission point is not so rapid as to preclude energy thermalization or partial equilibration along the way. One can expect that the evaporation of particles from the composite system may well depend on the time available between impact and scission. Therefore the good match in CE multiplicities for the two entrance channels is also a good indication that similar time scales are involved in these fissionlike processes. Such a conclusion is further supported when we compare ^{1}H and ^{4}He multiplicities for the ER's in the next section. As we will see, the ER multiplicities are much larger.

The statistical model (GANES) calculations used to obtain the particle multiplicities were made with two free parameters: (1) the deformation of the composite system and (2) the fractional excitation energy lost by deformation and/or particle emission prior to the emission of the particle of interest. The deformation of the composite system plays a key role in the calculations of the anisotropy in the particle angular distributions as well as in the energy spectra. The fractional energy loss ($\langle$FEL$\rangle$) affects the temperature of the emitters and thus the slope on the high energy side of the particle spectra [31].

Table I lists the statistical model parameters used to derive the CE particle multiplicities for 640 MeV ^{86}Kr as well as those for 337 MeV ^{40}Ar. The Cassini [31] deformation parameter $\tilde{\epsilon}$ and the $\langle$FEL$\rangle$ were optimized so that both the experimental particle energies and their angle-dependent intensities were duplicated by the calculations. (See [9] and [5] for more details on the statistical model fits to the energy spectra.) As noted earlier, the value of J_{rms} is obtained from the experimental cross sections. That it is higher ($97\hbar$) for the ^{86}Kr reaction reflects the larger fragment cross sections due to the presence of a DIR component in the measured fission cross section. The deformation parameter is the same for both entrance channels (as is the associated axis ratio d_1/d_2). This value of $\tilde{\epsilon}$ was found necessary to reproduce the in-plane–out-of-plane fragment-particle anisotropies as well as the particle energies. This large axis ratio of 2.8 indicates a very deformed nucleus. It is larger than that calculated by the rotating liquid drop model [19] for a saddle point equilibrium shape and suggests the presence of a dinuclear complex moving along its way to fission.

Also given in Table I are the ratios of the perpendicular and parallel moments of inertia to that for a spherical nucleus. These values are determined by $\tilde{\epsilon}$ and thus are not independent variables. This is also the case for the evaporation barriers, B_{min} and B_{max}. The maximum barrier is the evaporation barrier for emission from the

TABLE I. Derived statistical properties of composite nucleus emitters that decay by fission.

	337 MeV ^{40}Ar + ^{nat}Ag [a]	640 MeV ^{86}Kr + ^{63}Cu
J_{rms} [b]	87	97
$\tilde{\epsilon}$ [c]	0.8	0.8
d_1/d_2 [c]	2.8	2.8
$\Im_\perp/\Im_0$ [d]	2.35	2.35
$\Im_\parallel/\Im_0$ [d]	0.54	0.54
B_{max} (MeV) [e]	16.7(α) 8.7(p)	16.7(α) 8.7(p)
B_{min} (MeV) [e]	12.9(α) 6.7(p)	12.9(α) 6.7(p)
B_{fus} (MeV) [f]	16.15(α) 8.7(p)	16.15(α) 8.7(p)
$\langle$FEL$\rangle$ [g]	0.15(α) 0.15(p)	0.15(α) 0.60(p)
τ^{FF}(MeV) [h]	2.9(α) 2.9(p)	2.9(α) 1.9(p)

[a]The listed quantities are taken from Ref. [8].
[b]Root-mean-square spin of the emitter. Derived from the measured FF cross section for the ^{40}Ar reaction; high value for the ^{86}Kr reaction probably reflects presence of DIR in measured fragment cross section.
[c]Cassini deformation parameter [22] and associated major/minor axis ratio of the deformed daughter nucleus.
[d]Moment of inertia perpendicular (parallel) to the symmetry axis compared to that of a sphere. These values are derived from the values selected for $\tilde{\epsilon}$.
[e]Barrier height for particle emission at the waist (max) or at the tip (min) of the prolate spheroid (values dependent on $\tilde{\epsilon}$). The average effective barrier is about B_{min} plus $\approx \frac{1}{2}(B_{max} - B_{min})$. This is substantially smaller than B_{fus}.
[f]Empirical barriers for fusion between cold nuclei [23].
[g]Fractional excitation energy lost due to particle emission or deformation prior emission of particle of interest. Uncertainties difficult to estimate and may be as large as the values listed.
[h]Mean temperature of the daughter nuclei. These values result from the values selected for $\langle$FEL$\rangle$.

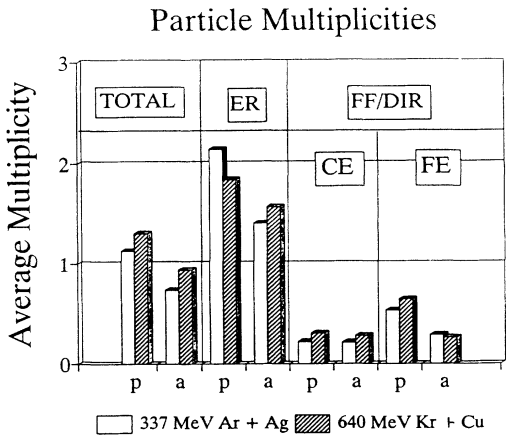

FIG. 5. Comparison of particle multiplicities (^{1}H = p, ^{4}He = α) for different sources produced in the reactions 337 MeV ^{40}Ar + ^{nat}Ag (open) and 640 MeV ^{86}Kr + ^{63}Cu (solid).

waist of a prolate system; the minimum is for emission from the tips. Barriers are listed for both ^{4}He (α) and ^{1}H (p) emissions. These shape-dependent barriers are well matched for these two reactions. For the ^{40}Ar reaction, a single value of $\langle$FEL$\rangle$ (hence temperature) was obtained for both ^{1}H and ^{4}He emission. This value is 0.15 and agrees with ^{4}He emission from the ^{86}Kr reaction. The apparent values of $\langle$FEL$\rangle$ (temperature), however, seem to differ for ^{1}H emission. For the ^{86}Kr reaction it is 0.60 (1.90 MeV), and for the ^{40}Ar reaction it was 0.15 (2.9 MeV). However, the uncertainty in the derived value of $\langle$FEL$\rangle$ for ^{1}H may be as large as the value itself, as the statistical model fits to the data have only small sensitivity to this parameter.

Overall, the good agreement between ^{1}H and ^{4}He multiplicities, and the statistical model parameters used to derive the multiplicities, indicates that the relaxation time is significantly shorter than the decay lifetime for these nuclei with substantial spins. Also, it would seem that the time to fission is longer than the lifetime of the composite nucleus for at least the first-step emission of a light particle.

B. ^{1}H and ^{4}He multiplicities for the ER's

ER particle multiplicities are reported in [10] for the ^{86}Kr reaction and in [5] for the ^{40}Ar reaction. A comparison of these multiplicities is presented in Fig. 5. The salient feature is their close agreement for the two channels; this gives strong evidence for equilibration.

One observes immediately from Fig. 5 that regardless of entrance channel, ER multiplicities are much larger than those from FF/DIR. This is due in small part to the greater amount of thermal excitation energy in the composite systems that result from the more central collisions and decay to ER's. It also reflects the change in binding energies for charged particles in the composite system and in the fragments; the light charged particles LCP's (as opposed to neutrons) are more tightly bound by the more neutron-rich fragments. Hence, LCP emission probabilities from the fragments are less than those for the ER's. Nevertheless, the multiplicities for fragment emission are larger than those for prescission emission for the FF/DIR class. These prescission multiplicities probably reflect restrictions from the lifetime of the fissioning nucleus. We also note that ^{1}H emission is the preferred light charged particle decay mode (except for composite emission) for all reaction classes independent of entrance channel. This results from the fact that the sum of barrier plus binding energy for ^{1}H is smaller than that for ^{4}He.

The major point in Fig. 5 is the good match of the two reaction systems, which indicates equilibration.

V. ER SUBSET CROSS SECTIONS FOR ^{1}H AND ^{4}He EMISSION

In the previous section we observed agreement between ER particle multiplicities that are averaged over the entire ER reaction group. However, the statistical model suggests that heavier ^{4}He particles may be preferentially emitted from a higher-spin zone than the protons [21]. This model assumes that particle emission is driven by the available phase space. The decay path that leads to the greatest number of states in the daughter nucleus is therefore the preferred exit channel. Thus ^{4}He, by virtue of its greater mass, on average removes more angular momentum than the lighter particles (e.g., $\approx 7\hbar$ for ^{4}He as opposed to $\approx 3\hbar$ for ^{1}H). For ^{4}He emission, this drives down the rotational energy of the daughter nucleus thus enhancing ^{4}He production from a high-spin emitter as compared to that for the lighter particles. The statistical model thus predicts that the different particles are preferentially emitted from different spin zones. Therefore one can imagine a group of parent nuclei for ^{4}He emission that is a subset of the entire ER group, i.e., that the cross section for this subset contains only the sources for ^{4}He particles. As indicated in the previous section, there is agreement in the overall particle multiplicities for the ER reaction class from the two matched entrance channels. The question now is, what is the situation for the subset cross sections? In other words, we can decompose the entire ER cross section into subsets and their associated ^{1}H and ^{4}He particle multiplicities; then by comparisons between entrance channels, we can obtain another demanding test for equilibration to complement those from the particle energy spectra and their angular distributions.

VI. DEFINITION OF THE SUBSET CROSS SECTION

In a previous paper [5] we have shown how one can utilize the combination of cross section data (singles, double coincidences, triple coincidences, etc.) for the ER reaction class. The analysis can be pursued at several different levels to obtain average subset cross sections and multiplicities for a given emitted particle (or combination of particles). In this paper we use the most simple of these approaches as an additional test for equilibration.

Consider the production of a set of products (A) which, on average, emit a sequence of $\langle n_a\rangle^4$He or $\langle m_p\rangle^1$H particles. Let σ_A be the cross section for producing this set; then the ^{4}He and ^{1}H singles cross sections σ_s^a and σ_s^p from this set can be written as

$$\sigma_s^\alpha(A) = \sigma_{A\alpha}\langle n_\alpha\rangle, \quad \sigma_s^p(A) = \sigma_{Ap}\langle m_p\rangle, \tag{6.1}$$

where $\sigma_{A\alpha}$ and σ_{Ap} are average subset cross sections for the products which emit ^{4}He and ^{1}H, respectively. The fact that the subset cross sections (σ_{Ap} and $\sigma_{A\alpha}$) in Eq. (6.1) may be different from σ_A allows the possibility that some ER's may not emit ^{4}He or ^{1}H and that the overlap between ^{4}He and ^{1}H emitters may not necessarily be complete.

For indistinguishable particles (e.g., α-α or p-p) the double coincidence cross sections can be evaluated from the following expressions:

$$\sigma_{\rm DC}^{aa}(A) = \sigma_{Aa}\langle n_a(n_a-1)\rangle,$$

$$\sigma_{\rm DC}^{pp}(A) = \sigma_{Ap}\langle m_p(m_p-1)\rangle, \quad \text{for } n,m>1, \tag{6.2}$$

while for distinguishable particles (e.g., p-α)

$$\sigma_{\rm DC}^{p\alpha}(A) = \sigma_{Ap\alpha}\langle m_p\rangle\langle n_a\rangle. \tag{6.3}$$

Here $\sigma_{Ap\alpha}$ denotes the average overlap between σ_{Ap} and σ_{Aa}, i.e., the subset cross section for products which on average emit n ^{4}He and m ^{1}H particles.

From Eqs. (6.1)–(6.3) it is clear that one can obtain values for the average subset cross sections ($\sigma_{A\alpha}$, σ_{Ap}, and $\sigma_{Ap\alpha}$) and the average multiplicities ($\langle m_p\rangle$ or $\langle n_\alpha\rangle$) if the singles and double coincidence cross sections (σ_s^a, σ_s^p, $\sigma_{\rm DC}^{\alpha\alpha}$, and $\sigma_{\rm DC}^{pp}$) can be fixed for a certain specified set of reactions.

For the case of ^{1}H from the 640 MeV ^{86}Kr + ^{63}Cu reaction, the simultaneous equations are

$$\sigma_s^p({\rm ER}) = 587 \text{ mb} = \sigma_{Ap}\langle m_p\rangle, \tag{6.4}$$

$$\sigma_{\rm DC}^{pp}({\rm ER}) = 894 \text{ mb} = \sigma_{Ap}\langle m_p\rangle\langle m_p-1\rangle, \tag{6.5}$$

from which is obtained $\sigma_{Ap} = 233$ mb and $\langle m_p\rangle = 2.5$. Equations similar to (6.4) and (6.5) can be written for ^{4}He emission. Once these multiplicities are known, the "overlap cross section" $\sigma_{Ap\alpha}$ may be evaluated from Eq. (6.3).

A. Comparison of experimental values

Values obtained for dimensionless subset cross sections and their associated multiplicities are listed in Table II for the reactions 337 MeV ^{40}Ar + $^{\rm nat}$Ag and 640 MeV ^{86}Kr + ^{63}Cu. For both entrance channels, these subset cross sections (particle multiplicities) are substantially smaller (larger) than those averaged over the entire ER cross section. This indicates that the entire ER spin range is not responsible for each particle's production, but that for each particle there are certain spin ranges that emphasize that particle's production. The general agreement in dimensionless subset cross sections and their multiplicities shown in Table II suggests that these quantities are equilibrium properties of the fused system. Poorer agreement is found for the ^{4}He subset cross sections. This probably reflects uncertainties in the measured cross sections rather than an entrance channel difference, because results from a similar analysis for ^{149}Tb* with excitation energies of 128 and 154 MeV *do* give agreement [11,12].

TABLE II. Dimensionless subset cross sections and multiplicities.

	337 MeV ^{40}Ar + $^{\rm nat}$Ag[a]	640 MeV ^{86}Kr + ^{63}Cu
$\sigma_{Ap}/\pi\lambda\!\!\!^{-2}$	3720 ±1100	3584 ±1025
$\langle m\rangle_p$	2.5 ±0.8	2.5 ±0.6
$\sigma_{A\alpha}/\pi\lambda\!\!\!^{-2}$	2700±800	4974 ±929
$\langle n\rangle_\alpha$	2.5 ±0.7	1.8 ±0.3
$\sigma_{Ap\alpha}/\pi\lambda\!\!\!^{-2}$	1670 ±600	1778 ±754

[a] Listed values are from Ref. [5].

The sum of σ_{Ap} and $\sigma_{A\alpha}$ is somewhat larger than that for the total reaction class $\sigma_{\rm ER}$ by 196 mb for the ^{86}Kr reaction and by 138 mb for the ^{40}Ar reaction. This leads to the conclusion that the subset cross sections for ^{1}H and ^{4}He production overlap and share some common parentage. The emitters in common for both particle types give rise to the overlap cross section, $\sigma_{Ap\alpha}$.

The measured value of this overlap cross section is 116 mb for the ^{86}Kr reaction and 154 mb for the ^{40}Ar reaction (with $\approx$ 30% error on each). These overlaps must be subtracted from the respective sum of the other two cross sections to obtain a corrected sum

$$\sigma_{\rm total} = \sigma_{Ap} + \sigma_{A\alpha} - \sigma_{Ap\alpha}. \tag{6.6}$$

Application of Eq. (6.6) gives for the ^{86}Kr (^{40}Ar) reaction $\sigma_{\rm total}$ = 440 ±112 mb (439 ±135 mb), which is consistent with $\sigma_{\rm ER}$ = 360 ±66 mb (455 ±55 mb).

Note that $\sigma_{Ap\alpha}$ is much smaller than that for σ_{Ap} or $\sigma_{A\alpha}$. In other words, most reactions take place in which one or the other particle is produced but not both. This is true for both entrance channels. As remarked earlier, these findings are not inconsistent with expectations of the statistical model that suggest preferential ^{4}He emission by systems that have larger angular momenta than those that emit ^{1}H. These subset cross sections in themselves do not allow us to assign their spin regions, but the relatively large angular anisotropies for ^{4}He and ^{4}He-^{4}He emission suggest that these particles are emitted by nuclei that on average have higher spins than those that emit ^{1}H.

VII. CONCLUSIONS

We have compared various experimental results for two entrance channel reactions: 337 MeV ^{40}Ar + $^{\rm nat}$Ag and 640 MeV ^{86}Kr + ^{63}Cu. The composite nuclei produced in these reactions have excitation energies of 194 MeV. It was shown in Figs. 1(c) and 1(d) that the spin region for ER's is essentially the same for both entrance channels. From this we conclude that the equilibrated composite nucleus (not the colliding nuclei) decides what is the limiting angular momentum for ER production above which fission takes over as the preferred decay path.

We have also examined light charged particle spectra for inclusive and exclusive reactions. All these particle spectra are distinctly Maxwellian in spectral shape. The inclusive c.m. ^{4}He energy spectra for both reactions generally agree in spectral shape and average energy. However, some deviations are found on the low energy sides of these spectra, which may be attributed to fragment emission. By contrast, the ^{4}He-^{4}He coincidence energy spectra agree for both the high and low energy particles; it is known [5] that ~86% of the coincidence cross section comes from composite nuclei that decay to ER's. This one dominant emission source accounts for the good

agreement in spectral shapes for these coincidence spectra. Furthermore, the average c.m. energies are nearly invariant with angle. We conclude that a long-lived intermediate nucleus has been formed and that there is no significant contribution from any fast prethermalization processes.

A gentle backward peaking in the inclusive and coincidence particle angular distributions gives a signature for a long-lived, rotating intermediate nucleus. Angular anisotropies, both in plane and out of plane, agree well for these two entrance channels. This is consistent with a common spin zone and for comparable shapes for the composite nuclei.

Energy spectra for ^{1}H, ^{2}H, and ^{4}He in coincidence with ^{4}He exhibit substantial shifts in energy with respect to statistical model calculations that employ cold fusion barriers for spherical nuclei. Such shifts suggest a hot, expanded nuclear stratosphere. These shifts are found to be extremely similar for these paired reactions; this result indicates a common shape evolution for the emitters as they cool. It shows that such a nuclear stratosphere (if indeed it is the cause) is an equilibrium feature of the composite nuclei. Anisotropies for in-plane and out-of-plane particle-particle angular distributions also agree; this points toward similar average spins, moments of inertia, and nuclear temperatures for these emitters.

Fragment-particle coincidence measurements also indicate extensive thermal and shape equilibration for the Tb* composite systems with high spins. Statistical model analysis of the light charged particles in coincidence with fragments gives evidence for strongly deformed composite nuclei. This deformation is required in statistical model calculations in order to reproduce both the observed particle energy spectra and anisotropy for in-plane–out-of-plane coincidence measurements. Statistical model parameters derived from data for the matched entrance channels also agree. Multiplicities for prefission, light charged particle emission generally, are in good agreement. This agreement indicates similar fission time scales between time of impact and scission. Postfission as well as prefission particle multiplicities are in good agreement.

For the ER reaction class, there is agreement for the various dimensionless cross sections and their associated particle multiplicities. This indicates that equilibrated composite nuclei control the decay probabilities for these exit channels. The observation of a rather small p-α coincidence rate (i.e., overlap cross section, $\sigma_{Ap\alpha}$) for all entrance channels strongly suggests that separate spin zones are mainly responsible for ^{1}H and ^{4}He emission. This is consistent with expectations of the statistical model which predicts ^{4}He to be emitted from nuclei with larger spins than those that emit ^{1}H.

From the above observations, we are led to the conclusion that the ^{149}Tb* composite nuclei, produced in these entrance channel reactions, exhibit extensive thermal and shape equilibration over a broad spin and excitation energy range. Even though the nuclear relaxation times and initial decay lifetimes are expected to be similar, we are lead to the conclusion that the driving force toward equilibration is still dominant.

ACKNOWLEDGMENTS

We thank our colleagues of the accompanying paper for the permission to present several additional experimental observations from that work. Helpful discussions with M. Kaplan are gratefully acknowledged. This work was supported by the Division of Nuclear Physics, Office of High Energy and Nuclear Physics, U.S. Department of Energy.

[1] M. Gonin, L. Cooke, K. Hagel, Y. Lou, J. B. Natowitz, R. P. Schmitt, S. Shlomo, B. Srivastava, W. Turmel, H. Utsunomiya, R. Wada, G. Nardelli, G. Nebbia, G. Viesti, R. Zanon, B. Fornal, G. Prete, K. Niita, S. Hannuschke, P. Gonthier, and B. Wilkins, Phys. Rev. C **42**, 2125 (1990).

[2] J. B. Natowitz, M. Gonin, K. Hagel, S. Shlomo, X. Bin, M. Gui, Y. Lou, D. Utley, T. Botting, R. K. Choudhury, L. Cooke, B. Hurst, D. O'Kelly, R. P. Schmitt, W. Turmel, H. Utsunomiya, G. Nebbia, D. Fabris, J. A. Ruiz, G. Nardelli, M. Poggi, R. Zanon, G. Viesti, R. H. Burch, F. Gramegna, G. Prete, D. Drain, B. Chambon, B. Cheynis, D. Guinet, X. C. Hu, A. Demeyer, C. Pasteur, A. Giorni, A. Lleres, P. Stassi, B. Viano, A. Menchaca Rocha, M. E. Brandan, and P. Gonthier, Nucl. Phys. **A538**, 263c (1992).

[3] T. Ericson, Adv. Phys. **9**, 423 (1960).

[4] A. E. Glassgold, W. Heckrotte, and K. Watson, Ann. Phys. (N.Y.) **6**, 1 (1959).

[5] R. Lacey, N. N. Ajitanand, J. M. Alexander, D. M. de Castro Rizzo, G. F. Peaslee, L. C. Vaz, M. Kaplan, M. Kildir, G. La Rana, D. J. Moses, W. E. Parker, D. Logan, M. S. Zisman, P. DeYoung, and L. Kowalski, Phys. Rev. C **37**, 2561 (1988).

[6] A. Gavron, A. Gayer, J. Boissevain, H. C. Britt, T.C. Awes, J. R. Beene, B. Cheynis, D. Drain, R. L. Ferguson, F. E. Obenshain, F. Plasil, G. R. Young, G. A. Petitt, and C. Butler, Phys. Rev. C **35**, 579 (1987).

[7] D. J. Hinde, D. Hilscher, H. Rossner, B. Gebauer, M. Lehmann, and M. Wilpert, Phys. Rev. C **45**, 1229 (1992).

[8] R. Lacey, N. N. Ajitanand, J. M. Alexander, D. M. de Castro Rizzo, G. F. Peaslee, L. C. Vaz, M. Kaplan, M. Kildir, G. La Rana, D. J. Moses, W. E. Parker, D. Logan, M. S. Zisman, P. DeYoung, and L. Kowalski, Phys. Rev. C **37**, 2540 (1988).

[9] J. Boger, Ph.D. thesis, Department of Chemistry, State University of New York at Stony Brook, 1992.

[10] J. Boger, J. M. Alexander, G. Auger, A. Elmaani, S. Kox, A. Narayanan, M. Kaplan, D. J. Moses, M. A. McMahan, P. A. DeYoung, C. J. Gelderloos, and G. Gilfoyle, accompanying paper, Phys. Rev. C **49**, 1576 (1994).

[11] W. E. Parker, Ph.D. thesis, Department of Chemistry, Carnegie Mellon University, 1989.

[12] W. E. Parker, M. Kaplan, D. J. Moses, J. M. Alexander, J. T. Boger, R. A. Lacey, and D. M. deCastro Rizzo, Nucl. Phys. (to be published).
[13] U. Jahnke, H. H. Rossner, D. Hilscher, and E. Holub, Phys. Rev. Lett. **48,** 17 (1981).
[14] C. Cabot, H. Gauvin, Y. Le Beyec, H. Delagrange, J. P. Dufour, Y Llabador, A. Fleury, and J. M. Alexander, Nucl. Phys. **A427**, 173 (1984).
[15] H. C. Britt, B. H. Erkkila, R. H. Stokes, H. H. Gutbrod, F. Plasil, R. L. Ferguson, and M. Blann, Phys. Rev. C **13**, 1483 (1976).
[16] F. Plasil, R. L. Ferguson, H. C. Britt, B. H. Erkkila, P. D. Goldstone, R. J. Stokes, and H. H. Gutbrod, Phys. Rev. C **18**, 2603 (1978).
[17] H. C. Britt, B. H. Erkkila, P. D. Goldstone, R. H. Stokes, B. B. Back, F. Folkmann, O. Christensen, B. Fernandez, J. D. Garrett, G. B. Hagemann, B. Herskind, D. C. Hillis, F. Plasil, R. L. Ferguson, M. Blann, and H. H. Gutbrod, Phys. Rev. Lett. **39**, 1458 (1977).
[18] T. Ethivignot, N. N. Ajitanand, C. J. Gelderloos, J. M. Alexander, E. Bauge, A. Elmaani, R. A. Lacey, P. Desesquelles, H. Elhage, A. Giorni, D. Heuer, S. Kox, A. Lleres, F. Merchez, C. Morand, D. Rebreyend, P. Stassi, J. B. Viano, F. Benrachi, B. Chambon, B. Cheynis, D. Drain, and C. Pastor, Nucl. Phys. **A545**, 347c (1992).
[19] S. Cohen, F. Plasil, and W. J. Swiatecki, Ann. Phys. (N.Y.) **8**, 557 (1974).
[20] J. Blatt and V. F. Weisskopf, *Theoretical Nuclear Physics* (Wiley, New York, 1952).
[21] T. Dossing, Licentiat thesis, University of Copenhagen, Denmark, 1977.
[22] N. N. Ajitanand, R. Lacey, G. F. Peaslee, E. Duek, and J. M. Alexander, Nucl. Instrum. Methods Phys. Res. A **243**, 111 (1986).
[23] L. C. Vaz and J. M. Alexander, Z. Phys. **A318**, 231 (1984).
[24] G. La Rana, D. J. Moses, W. E. Parker, M. Kaplan, D. Logan, R. Lacey, John M. Alexander, and R. J. Welberry, Phys. Rev. C **35**, 373 (1987).
[25] G. Batko and O. Citravese, Phys. Rev. **C37**, 2647 (1988).
[26] R. Lacey, N. N. Ajitanand, J. M. Alexander, D. M. de Castro Rizzo, P. DeYoung, M. Kaplan, L. Kowalski, G. La Rana, D. Logan, D.J. Moses, W. E. Parker, G. F. Peaslee, and L. C. Vaz, Phys. Lett. B **191**, 253 (1987).
[27] J. R. Huizenga, A. N. Behkami, I. M. Govil, W. U. Schroder, and J. Toke, Phys. Rev. C **40**, 668 (1989).
[28] J. M. Alexander, G. Auger, M. Kaplan, L. Kowalski, R. Lacey, G. La Rana, M. T. Magda, and G. F. Peaslee, in *Proceedings of the Symposium "Nuclear Dynamics and Nuclear Disassembly*, Dallas, Texas, 1989," edited J. B. Natowitz (World Scientific Publishers, Singapore, 1989), p. 211.
[29] W. E. Parker, M. Kaplan, D. J. Moses, G. La Rana, D. Logan, R. Lacey, J. M. Alexander, D. M. de Castro Rizzo, P. DeYoung, R. J. Welberry, and J. T. Boger, Phys. Rev. C **44**, 774 (1991).
[30] G. F. Peaslee, Ph.D. thesis, Department of Chemistry, SUNY Stony Brook, 1987.
[31] V. V. Pashkevich, Nucl. Phys. **A169**, 275 (1971).